Crystal Structures of Native and Inactivated cis-3-Chloroacrylic Acid Dehalogenase. Structural Basis for Substrate Specificity and Inactivation by (R)-Oxirane-2-Carboxylate

Jong, René M. de; Bazzacco, Paola; Poelarends, Gerrit J.; Johnson, Jr.; Kim, Yoon Jae; Burks, Elizabeth A.; Serrano, Hector; Thunnissen, Andy-Mark W.H.; Whitman, Christian P.; Dijkstra, Bauke W.

Published in:
The Journal of Biological Chemistry

DOI:
10.1074/jbc.M608134200

Publication date:
2007

THE JOURNAL OF BIOLOGICAL CHEMISTRY VOL. 282, NO. 4, pp. 2440–2449, January 26, 2007

Crystal Structures of Native and Inactivated *cis*-3-Chloroacrylic Acid Dehalogenase

*STRUCTURAL BASIS FOR SUBSTRATE SPECIFICITY AND INACTIVATION BY (R)-OXIRANE-2-CARBOXYLATE**

Received for publication, August 24, 2006, and in revised form, October 26, 2006 Published, JBC Papers in Press, November 22, 2006, DOI 10.1074/jbc.M608134200

René M. de Jong[‡1], Paola Bazzacco[‡], Gerrit J. Poelarends[§], William H. Johnson, Jr.[¶], Yoon Jae Kim[¶], Elizabeth A. Burks[¶], Hector Serrano[¶], Andy-Mark W. H. Thunnissen[‡], Christian P. Whitman[¶2], and Bauke W. Dijkstra[‡3]

From the [‡]Laboratory of Biophysical Chemistry and [§]Department of Biochemistry, Groningen Biomolecular Sciences and Biotechnology Institute, University of Groningen, Nijenborgh 4, 9747 AG Groningen, The Netherlands and the [¶]Division of Medicinal Chemistry, College of Pharmacy, The University of Texas, Austin, Texas 78712-1074

The bacterial degradation pathways for the nematocide 1,3-dichloropropene rely on hydrolytic dehalogenation reactions catalyzed by *cis*- and *trans*-3-chloroacrylic acid dehalogenases (*cis*-CaaD and CaaD, respectively). X-ray crystal structures of native *cis*-CaaD and *cis*-CaaD inactivated by (*R*)-oxirane-2-carboxylate were elucidated. They locate four known catalytic residues (Pro-1, Arg-70, Arg-73, and Glu-114) and two previously unknown, potential catalytic residues (His-28 and Tyr-103′). The Y103F and H28A mutants of these latter two residues displayed reductions in *cis*-CaaD activity confirming their importance in catalysis. The structure of the inactivated enzyme shows covalent modification of the Pro-1 nitrogen atom by (*R*)-2-hydroxypropanoate at the C3 position. The interactions in the complex implicate Arg-70 or a water molecule bound to Arg-70 as the proton donor for the epoxide ring-opening reaction and Arg-73 and His-28 as primary binding contacts for the carboxylate group. This proposed binding mode places the (*R*)-enantiomer, but not the (*S*)-enantiomer, in position to covalently modify Pro-1. The absence of His-28 (or an equivalent) in CaaD could account for the fact that CaaD is not inactivated by either enantiomer. The *cis*-CaaD structures support a mechanism in which Glu-114 and Tyr-103′ activate a water molecule for addition to C3 of the substrate and His-28, Arg-70, and Arg-73 interact with the C1 carboxylate group to assist in substrate binding and polarization. Pro-1 provides a proton at C2. The involvement of His-28 and Tyr-103′ distinguishes the *cis*-CaaD mechanism from the otherwise parallel CaaD mechanism. The two mechanisms probably evolved independently as the result of an early gene duplication of a common ancestor.

The *cis*- and *trans*-3-chloroacrylic acid dehalogenases (*cis*-CaaD and CaaD)[4] catalyze the cofactor-independent hydrolytic dehalogenation of, respectively, the *cis*- and *trans*-isomers of 3-chloroacrylic acid (**1** and **2**, Scheme 1) to produce malonate semialdehyde (**5**) and HCl (1–3). Both reactions may be initiated by the attack of water at C3 to form an enzyme-stabilized enediolate intermediate (**3**). Subsequent ketonization of **3** with protonation at C2 generates a chlorohydrin intermediate (**4**), which can collapse by direct expulsion of the chloride to afford **5** (1, 4, 5). Alternatively, ketonization of **3** can result in chloride loss and the formation of the enol intermediate, **6**, which tautomerizes to afford **5**. The two enzymes are found in bacterial pathways that convert the *cis*- and *trans*-isomers of 1,3-dichloropropene, used as nematocides, to acetaldehyde (**7**) and carbon dioxide (6).

The *cis*- and *trans*-3-chloroacrylic acid dehalogenases have low sequence identity (~20%) and different oligomerization states (1–3). CaaD is a heterohexamer consisting of three 75-residue α-chains and three 70-residue β-chains, whereas *cis*-CaaD forms a homotrimer of three identical 149-residue polypeptide chains, which can be considered as the fusion product of a CaaD α- and β-chain (2, 3, 5). As a result, the two enzymes have been classified in two different families in the tautomerase superfamily, with each being related to 4-oxalocrotonate tautomerase (7–9). Yet, the differences in catalytic efficiency are only modest, and major elements of the catalytic mechanisms are conserved. In both, a glutamate residue (Glu-114 in *cis*-CaaD and αGlu-52 in CaaD) is proposed to function as a general base catalyst to activate a water molecule for attack at C3 (of **1** or **2**) and the N-terminal proline (Pro-1 in *cis*-CaaD and βPro-1 in CaaD) is believed to provide a proton at C2. Two

* This work was supported in part by United States Public Health Services Grant GM 65324. The mass spectrometry described in this paper was carried out in the Analytical Instrumentation Facility Core housed in the College of Pharmacy at the University of Texas at Austin and supported by Center Grant ES07784. The costs of publication of this article were defrayed in part by the payment of page charges. This article must therefore be hereby marked "*advertisement*" in accordance with 18 U.S.C. Section 1734 solely to indicate this fact.

The atomic coordinates and structure factors (code 2FLZ and 2FLT) have been deposited in the Protein Data Bank, Research Collaboratory for Structural Bioinformatics, Rutgers University, New Brunswick, NJ (http://www.rcsb.org/).

[1] Supported by a long-term fellowship of the Human Frontier Science Program Organization and a Veni grant of the Netherlands Foundation for Chemical Science.

[2] To whom correspondence may be addressed: Division of Medicinal Chemistry, College of Pharmacy, The University of Texas, Austin, TX 78712-1074. Tel.: 521-471-6198; Fax: 512-232-2606; E-mail: whitman@mail.utexas.edu.

[3] To whom correspondence may be addressed. Tel.: 31-50-363-4381; Fax: 31-50-363-4800; E-mail: B.W.Dijkstra@rug.nl.

[4] The abbreviations used are: *cis*-CaaD and CaaD, *cis*- and *trans*-3-chloroacrylic acid dehalogenase, respectively; F_o and F_c, observed and calculated structure factor amplitudes, respectively; MSAD, malonate semialdehyde decarboxylase; r.m.s.d., root-mean-square deviation.

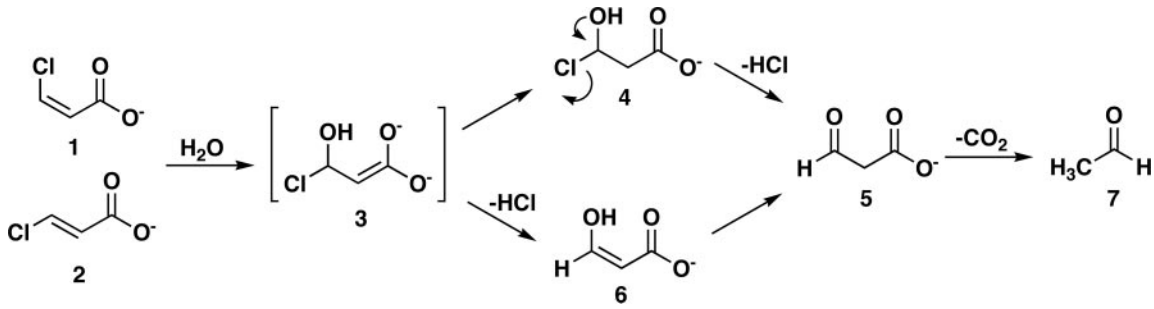

SCHEME 1

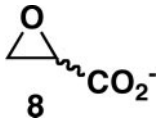

STRUCTURE 1

arginine residues (Arg-70 and Arg-73 in *cis*-CaaD and αArg-8 and αArg-11 in CaaD) are proposed to interact with the C1 carboxylate group, aligning the substrate in the active site and drawing electron density away from C3 (1, 3–5). Such an interaction would generate a partial positive charge at C3 and facilitate the addition of water. The conservation of key functionalities suggests that the two enzymes are related by divergent evolution from a common ancestor.

Nevertheless, recent kinetic and mechanistic work has uncovered two subtle differences. First, the activation of the water molecule likely requires additional residues in *cis*-CaaD (1). Mutation of Glu-114 to a glutamine produces a partially active mutant protein, whereas the αE52Q mutant of CaaD has no detectable activity, even after a prolonged incubation period. Second, only *cis*-CaaD is irreversibly inhibited by the (*R*)-oxirane-2-carboxylate (**8**) due to covalent modification of Pro-1 (10). The (*S*)-enantiomer is a weak competitive inhibitor of *cis*-CaaD and both enantiomers competitively inhibit CaaD (10) (Structure 1).

To delineate the structural basis for the isomer-specific dehalogenation reaction and the stereospecificity of the inactivation reaction, crystal structures of the native *cis*-CaaD and *cis*-CaaD inactivated by (*R*)-**8** were obtained. They confirm the trimeric nature of *cis*-CaaD and pinpoint the roles of Pro-1, Arg-70, Arg-73, and Glu-114. The assisting roles of His-28 and Tyr-103′ in activation of, respectively, the substrate and nucleophilic water molecule for catalysis, suggested by the structures, are supported by site-directed mutagenesis. It can also be inferred that His-28 plays a central role in positioning (*R*)-**8** for alkylation of Pro-1 and, along with Tyr-103′, is a determinant of the substrate specificity of the enzyme. The crystallographic observations fully support the proposal that *cis*-CaaD and CaaD form two separate evolutionary lineages that followed the independent duplication of a 4-oxalocrotonate tautomerase-like sequence.

EXPERIMENTAL PROCEDURES

Materials—All reagents, buffers, and solvents were obtained from Sigma-Aldrich, Fisher Scientific, Spectrum Laboratory Products (New Brunswick, NJ), or EM Science (Cincinnati, OH), unless noted otherwise. A literature procedure was used for the synthesis of (*R*)-**8** (11). The sources for the components of Luria-Bertani media, the enzymes and reagents used in the molecular biology procedures, and the strains used for cloning and overproducing *cis*-CaaD and the mutant proteins have been reported elsewhere (1, 10). The Amicon concentrator and the YM10 ultrafiltration membranes were obtained from Millipore Corp. (Bedford, MA). Oligonucleotides for DNA amplification and sequencing were synthesized by Genosys (The Woodlands, TX).

General Enzymology Methods—General procedures for cloning and DNA manipulation were performed as described elsewhere (12). The wild-type *cis*-CaaD and the mutant proteins were purified to homogeneity, as assessed by SDS-PAGE, according to a published procedure (1, 10). Protein was analyzed by SDS-PAGE on gels containing 15% polyacrylamide (13). The gels were stained with Coomassie Brilliant Blue. Protein concentrations were determined by the method of Waddell (14). The native molecular masses of the mutant proteins were determined by gel filtration on a Superose 12 column (Amersham Biosciences) using the Waters 501/510 high-pressure liquid chromatography system.

Crystallization and Structure Determination of Inactivated cis-CaaD—*cis*-CaaD was covalently inactivated by incubating the enzyme with a 25-fold excess of (*R*)-**8** for 4 h, after diluting the protein solution to 0.5 mg/ml to prevent overheating. Crystals of inactivated *cis*-CaaD were obtained from 2-μl hanging drops consisting of equal amounts of protein solution (10 mg/ml) and well solution containing 1.6 M potassium sodium phosphate and 100 mM HEPES buffer, pH 7.5. Thin hexagonal shaped crystals of 1.5 μm grew in a few days. A diffraction data set to 2.1-Å resolution was collected in-house on a MacScience image plate system using CuK_α radiation from a rotating anode generator. The data were processed using DENZO and SCALEPACK (15). The crystals belong to the space group $P6_3$ with cell constants $a = b = 59.5$ Å, and $c = 57.9$ Å. The asymmetric unit contains one monomer of 149 residues, of which the 22 C-terminal residues were not resolved in the electron density map.

Molecular replacement solutions were obtained with the program AMORE available in CCP4 (16, 17). A search model was constructed using the atomic coordinates of one heterodimer subunit (composed of an α and a β chain) from the *Pseudomonas pavonaceae* 170 heterohexameric CaaD (PDB code 1S0Y) (5). All residues were changed to alanines except for the proline and glycine residues. Rotation and translation func-

TABLE 1
Data collection and refinement statistics

	Native *cis*-CaaD	Inactivated *cis*-CaaD
Data statistics		
Space group	$P2_13$	$P6_3$
No. chains/asymmetric unit	3	1
Unit cell (Å)	$a = b = c = 141.4$	$a = b = 59.5$ $c = 57.9$
Resolution (Å)	40-2.75	30-2.1
R_{sym} (%) overall (outer shell)[a]	9.3 (35.9)	10.3 (35.5)
Completeness (%) overall (outer shell)	99.9 (100.0)	99.9 (100.0)
I/σ overall (outer shell)	19.2 (3.5)	19.8 (5.5)
Reflections total (unique)	165,665 (23,148)	61,304 (6,850)
Refinement		
Total atoms/water/SO_4	3,470/17/3	975/61/0
R/R_{free}[b]	23.3/26.3	20.2/23.0
r.m.s.d. bonds (Å)/angles (°)	0.08/1.35	0.07/1.32
r.m.s.d. B (Å^2) (main chain/side chain)	1.19/2.10	1.41/1.79
Ramachandran plot (%) (favored/allowed/generously allowed/disallowed)	93.9/6.1/0.0/0.0	96.0/3.0/1.0/0.0

[a] $R_{sym} = \Sigma|I - \langle I\rangle|/\Sigma I$, where I is the observed intensity and $\langle I\rangle$ the average intensity.
[b] R based on 95% of the data used in the refinement. R_{free} = R based on 5% of the data withheld from the cross-validation test.

tions were calculated using the data between 10- and 4-Å resolution. The molecular replacement yielded the position and orientation of a single monomer in the asymmetric unit. Refinement of the solutions by AMORE gave a correlation coefficient of 0.19 and an *R*-factor of 43.6%. The electron-density maps at this stage were not interpretable, but density was observed extending from some alanines of the search model. A σA-weighted map (18) calculated from the refined solutions from AMORE was used in a density-modification and phase-extension procedure using the prime-and-switch method available in the program RESOLVE (19). This improved the overall figure of merit from 0.24, after calculation of the starting map, to 0.52 in the final cycle of the density modification procedure. The resulting σA-weighted maps from RESOLVE showed improved electron density for the amino acid side chains and allowed identification of the N-terminal proline residue in the monomer of *cis*-CaaD. Manual building of side chains and missing main-chain atoms were subsequently alternated with simulated annealing and minimization runs in CNX (Accelrys Inc.). The program RESOLVE was used to obtain the most unbiased maps for model building, until σA-weighted $2F_o - F_c$ maps were of superior quality. The structure was built using QUANTA (Accelrys Inc.) and XtalView (20). Coordinates for the covalent adduct were based on 2-hydroxypropanoate and minimized in QUANTA (Accelrys Inc.), and its parameters were generated using the Hic-Up server (21). The quality of the final model was analyzed with PROCHECK (22). A summary of the data collection statistics, the refinement statistics, and geometric quality of the models is given in Table 1.

Crystallization and Structure Determination of Native cis-CaaD—Crystals of native *cis*-CaaD were obtained from 2-μl hanging drops consisting of equal amounts of protein solution (10 mg/ml) and well solution containing 10% (v/v) 2-propanol, as a precipitant, 100 mM phosphate-citrate buffer, pH 4.2, and 0.2 M Li_2SO_4. Cubes of 0.1 mm^3 grew within a few days. A diffraction data set to 2.75-Å resolution was collected at the ID14-2 beamline at the European Synchrotron Radiation Facility, Grenoble, France. The data were processed using DENZO and SCALEPACK (15). The crystal belonged to the space group $P2_13$ with cell parameters $a = b = c = 141.4$ Å. The asymmetric unit contains three monomers made up of 149 residues each. Short segments (2–3 residues) of the C termini were not resolved in the electron-density map.

Molecular replacement solutions were obtained with the program AMORE available in CCP4 (16, 17). A search model was constructed from the atomic coordinates of a *cis*-CaaD monomer inactivated by (*R*)-**8** with the coordinates of the covalent adduct removed. Rotation and translation functions were calculated using data between 15- and 3-Å resolution. The molecular replacement yielded the position and orientation of three monomers in the asymmetric unit. Refinement of the solutions by AMORE (16, 17) gave a correlation coefficient of 0.85 and an *R*-factor of 29%. Electron-density maps were further improved using the program DM available in CCP4 (17). The structure was built as described above for the inactivated *cis*-CaaD. A summary of the refinement statistics and geometric quality of the models is given in Table 1. Docking of **1** and **2** in the active sites of *cis*-CaaD and CaaD, respectively, was carried out manually using the program XtalView (20).

Construction, Expression, and Characterization of the H28A, Y103F, and Y103F/E114Q Mutants of cis-CaaD—The three mutant genes were generated by overlap extension PCR (23) using the plasmid pCC5 (1) as the template. The oligonucleotides, 5′-ATA**CATATG**CCGGTTTATATGGTTTAC-3′ and 5′-CAT**GGATCC**CTAGGTGCGAGAGACGTCCACGTT-3′ were used as the forward and reverse external primers, respectively. The forward primer contains an NdeI restriction site (in bold), and the reverse primer has a BamHI restriction site (in bold). For the H28A mutant, the internal PCR primers were oligonucleotides 5′-ATCACCGACGCGGCCAGGGGACTG-3′ and 5′-CAGTCCCCTGGCCGCGTCGGTGAT-3′. For the Y103F mutant, the internal PCR primers were oligonucleotides 5′-CACATCTGGGTCTTCTTCGGCAGA-3′ and 5′-CTCGCCGAAGAAGACCCAGATGTG-3′. For the Y103F/E114Q mutant, the internal PCR primers were oligonucleotides 5′-TGGGTCTTCTTCGGCGAGATGCCCGCCCAGCAGATGGTGCAGTACGGCC-3′ and 5′-GGCCGTACTGCACCATCTGCTGGGCGGGCATCTCGCCGAAGAAGACCCA-3′. The codons used to introduce the mutations are underlined. The amplification mixtures contained the appropriate synthetic primers, the deoxynucleotide triphosphates, the appropriate template DNA

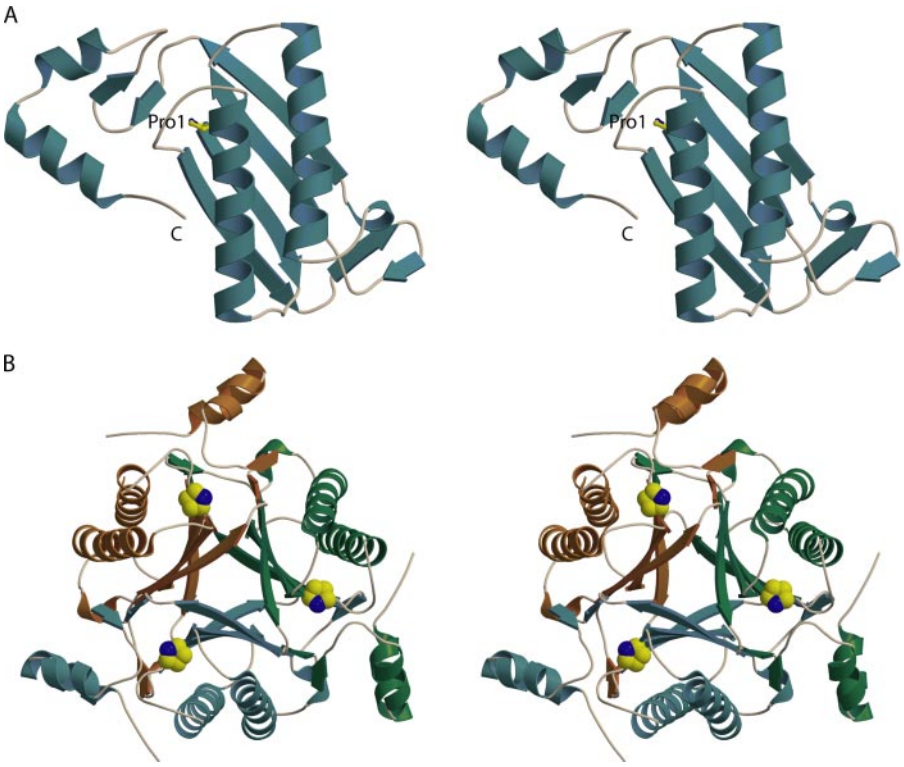

FIGURE 1. **Stereo views of (*A*) the monomeric and (*B*) the trimeric structure of *cis*-CaaD.** The catalytic Pro-1 is shown in *ball-and-stick* (*A*) and Corey-Pauling-Koltun (*B*) representation. The figures were made using MOLSCRIPT and RASTER3D (24, 25).

(~100 ng), and the PCR reagents supplied in either the Taq DNA polymerase system (H28A and Y103F) or the Expand High Fidelity PCR system (Y103F/E114Q, F. Hoffmann-La-Roche Ltd., Basel, Switzerland). The restriction sites NdeI and BamHI, introduced during the amplification reaction, were used to clone the purified PCR products into plasmid pET-3b or pET-3c for overexpression of the mutant proteins. The cloned genes were sequenced to verify that only the desired mutation had been introduced during the PCR. Subsequently, the mutant enzymes were expressed in *Escherichia coli* strain BL21-Gold(DE3) and purified to homogeneity (as assessed by SDS-PAGE) using the protocol described for wild type (1). The yields (ranging from 10 to 40 mg of homogeneous protein per liter of cell culture) were slightly diminished from those typically obtained for wild type (~50–70 mg/liter). The elution times for the three mutant proteins and the wild-type *cis*-CaaD are comparable (~34 min at a flow rate of 0.4 ml/min) during gel-filtration chromatography, indicating that the homotrimeric structures of the mutant proteins are intact and that global structural changes had not occurred as a result of the mutations.

Mass Spectrometric Characterization of the Mutant Proteins—The masses of the three *cis*-CaaD mutants were determined using an LCQ electrospray ion trap mass spectrometer (ThermoFinnigan, San Jose, CA), housed in the Analytical Instrumentation Facility Core in the College of Pharmacy at the University of Texas at Austin. The protein samples were made up as described elsewhere (3). The observed monomer masses were 16,556 Da (calc. 16,556 Da) for H28A, 16,606 Da (calc. 16,606 Da) for Y103F, and 16,605 Da (calc. 16,605 Da) for Y103F/E114Q. Electrospray ionization mass spectrometry analysis indicated that the subunit had the expected mass and was not blocked by the initiating formylmethionine.

Kinetic Characterization and ^1H NMR Spectroscopic Detection of cis-CaaD Activity—*cis*-CaaD activity was determined at 22 °C by following the absorbance decrease at 224 nm, corresponding to the hydration of **1** ($\epsilon = 2900\ \text{M}^{-1}\ \text{cm}^{-1}$), for 1 min (wild type and Y103F) or 10 min (E114Q and H28A) (1). Absorbance data were obtained on a Hewlett Packard 8452A Diode Array spectrophotometer. The reported kinetic parameters are a numerical average of multiple runs. For the NMR samples, an amount of **1** (4 mg, ~0.04 mmol) dissolved in Me_2SO-d_6 (30 μl) was added to 100 mM Na_2HPO_4 buffer (0.6 ml, pH ~9) and placed in an NMR tube. The pH of the reaction mixture was adjusted to 9.5. Subsequently, enzyme (~1.2 mg made up in 20 mM Na_2HPO_4 buffer, pH 8.0) was added to the reaction mixture. The reaction mixture was examined at 17 or 22 h (as noted in the text), and the amount of product was estimated by integration of the signals corresponding to **1**, **5**, **7**, and the corresponding hydrates (1). NMR spectra were recorded in 100% H_2O on a Varian Unity INOVA-500 spectrometer as described previously (1).

RESULTS AND DISCUSSION

Structure of the Native cis-CaaD—The native *cis*-CaaD crystal structure was solved to 2.75-Å resolution by molecular replacement methods and refined to R and R_{free} values of 23.3% and 26.3%, respectively. The asymmetric unit contains three monomers. Each monomer consists of a four-stranded β-sheet that is formed by the anti-parallel interaction of a pair of two-stranded parallel β-sheets (Fig. 1*A*). Two α-helices, each spanning the two strands of the parallel β-sheets, lie anti-parallel to each other in the concave side of the β-sheet plane. Hence, each monomer is made up of two β-α-β structural motifs that are characteristic of the tautomerase superfamily (7–9).

The three monomers in the asymmetric unit superimpose with root-mean-square deviation (r.m.s.d.) values of ~0.4 Å for 129 equivalent C_α atoms (out of a total of 149 amino acids). Each of the three monomers forms an independent barrel-like trimer by rotation around one of the crystallographic 3-fold rotation axes in the crystal (Fig. 1*B*). Interactions between the monomers are mediated by the edges of the four-stranded β-sheets and are mainly hydrophobic in nature. Each β-sheet further contributes polar residues that interact with each other and with three water molecules in

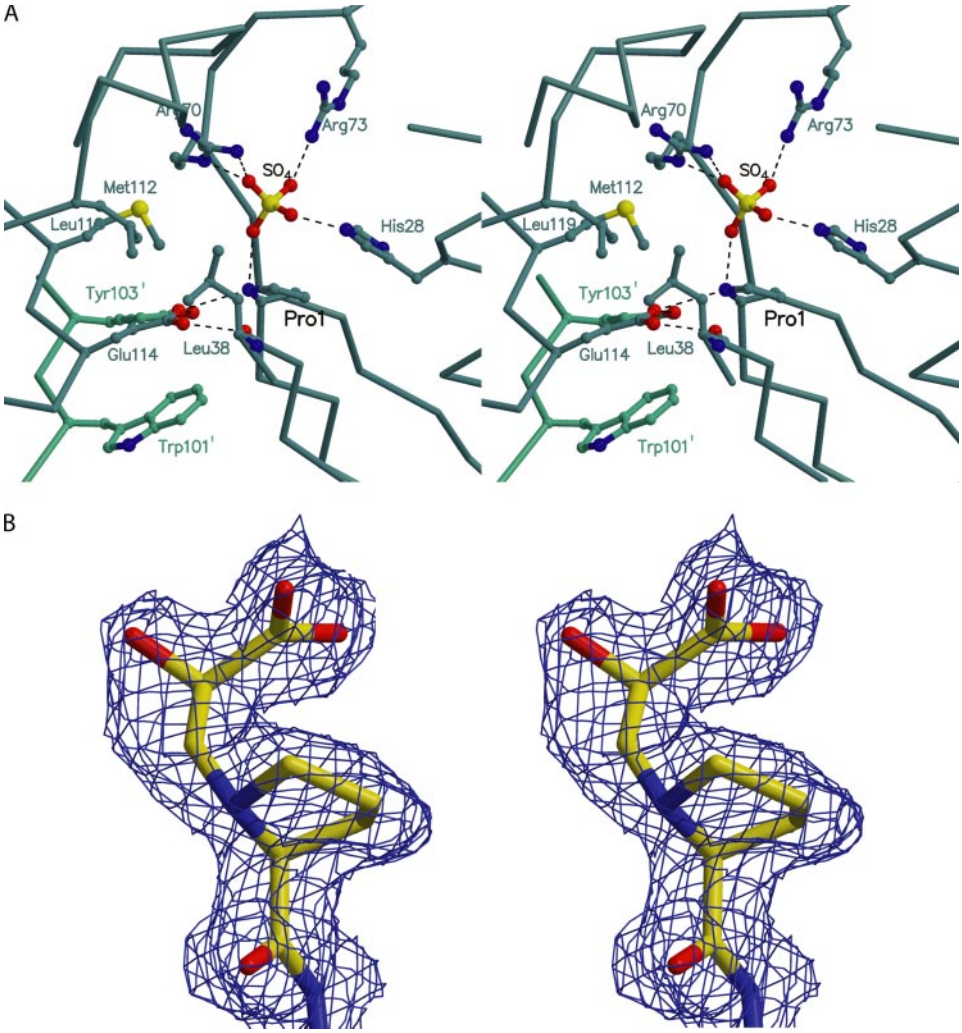

FIGURE 2. **Detailed overview of the structure of native *cis*-CaaD and the final electron density of the covalent adduct in the structure of inactivated *cis*-CaaD.** *A*, close-up stereo view of the active site of the native enzyme showing the interactions between the phosphate/sulfate ion and the two arginines (Arg-70 and Arg-73) and histidine (His-28). Residues are labeled by their chain color, except Pro-1, which is labeled in *black*. *B*, stereo view of the final $2F_o - F_c$ electron-density map contoured at 1.0 σ from XtalView (20) covering the proline and the covalently bound (*R*)-2-hydroxypropanoate adduct, clearly showing the tetrahedral conformations at the prolyl nitrogen and C2 of the adduct. The figures were prepared with MOLSCRIPT (*A*) (24) and RASTER3D (*A* and *B*) (24, 25).

the central cavity of the trimer. Additional monomer-monomer interactions are provided by two small β-hairpin structures near the termini of the central β-sheet and the two C-terminal α-helices (Fig. 1, *A* and *B*).

Active Site of Native cis-CaaD—cis-CaaD contains three active sites with the catalytically important N-terminal proline buried in the interior of a monomer on one side of the trimer (Fig. 1*B*). The Pro-1 nitrogen interacts with one of the oxygen atoms of a sulfate ion, or possibly a phosphate ion, that is bound in the active site cavity (Fig. 2*A*). Both ions were present in the crystallization solution. The prolyl nitrogen atom interacts with one of the sulfate/phosphate oxygen atoms. The other three oxygen atoms of the sulfate/phosphate ion have electrostatic and hydrogen-bonding interactions with two arginines, Arg-70 and Arg-73, a positively charged histidine, His-28, and Thr-34 (not shown). The prolyl nitrogen atom further interacts with one of the side-chain oxygen atoms of the catalytic base, Glu-114, which is stacked between Leu-119 and Trp-101′ from a neighboring monomer.[5] The same oxygen atom of Glu-114 interacts with the side-chain hydroxyl group of Tyr-103′, also from a neighboring monomer. The other carboxylate oxygen of Glu-114 interacts with the backbone carbonyl oxygen of Leu-38, suggesting that the side chain of Glu-114 is protonated. As such, Glu-114 cannot function as the water-activating catalytic base in the hydration reaction catalyzed by *cis*-CaaD. Such a protonation state of the glutamate, however, could be an artifact of the low pH at which the native enzyme was crystallized.

Comparison of cis-CaaD with Tautomerase Superfamily Members—cis-CaaD represents one of the five presently known families identified as constituents of the tautomerase superfamily (1, 2, 7–9, 26, 27). The other four families, represented by their title enzymes, are the 5-(carboxymethyl)-2-hydroxymuconate isomerase (28), 4-oxalocrotonate tautomerase (26, 29), macrophage migration inhibitory factor (30), and malonate semialdehyde decarboxylase (MSAD) families (27). *cis*-CaaD has been classified in a separate tautomerase family, the *cis*-CaaD family, because of the absence of significant sequence identity with known members of the other four families (1). The *trans*-specific CaaD, however, belongs to the 4-oxalocrotonate tautomerase family.

Like 5-(carboxymethyl)-2-hydroxymuconate isomerase, macrophage migration inhibitory factor, and MSAD, *cis*-CaaD is a trimer constructed from monomers containing two adjacent β-α-β structural motifs, which run in opposite directions (31–33). A structural alignment shows that the monomer structures of the four enzymes superimpose with r.m.s.d. values of 1.2 Å for 39 C_α atoms out of a total of 114–147 amino acids. These C_α atoms are located in the four β-strands and the second α-helix that build the central core of the monomers. The low number of matching C_α atoms reflects the structural differences found in the loop that connects the first and second β-α-β structural motif, and the C terminus. Of the four, the

[5] The unprimed and primed residues come from different monomers of *cis*-CaaD.

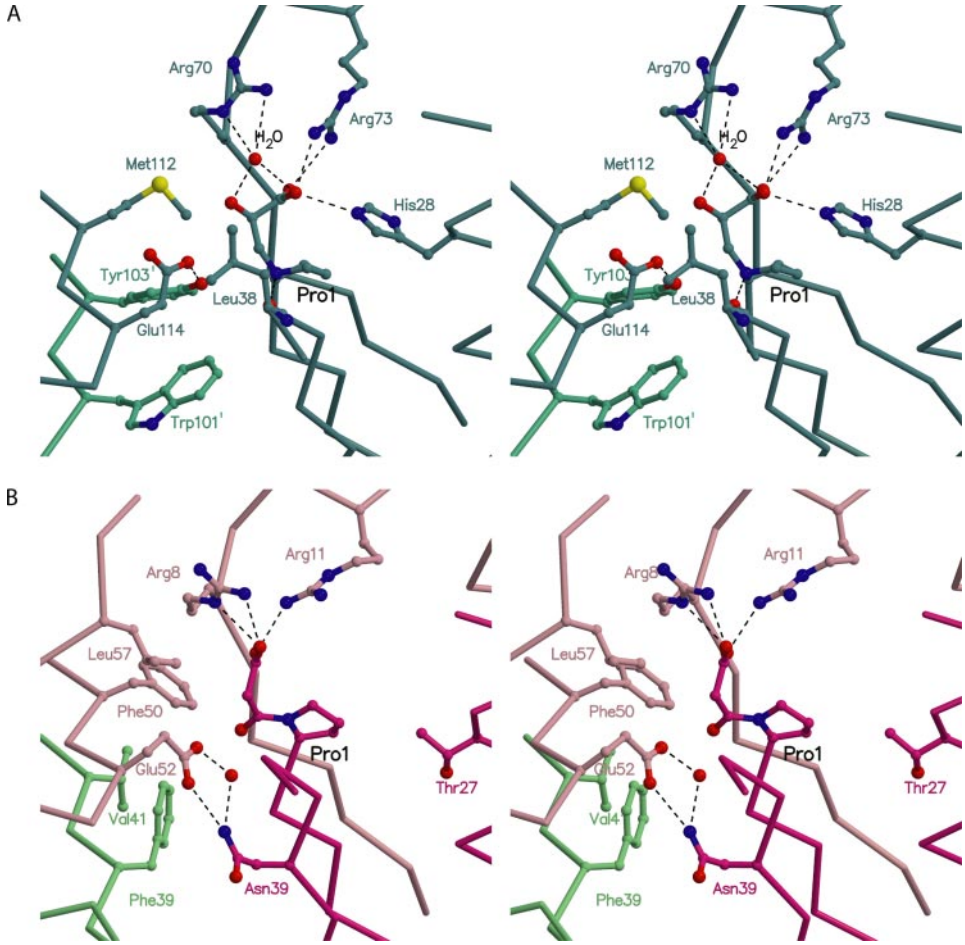

FIGURE 3. **Detailed overviews of the active sites of inactivated *cis*-CaaD and CaaD.** *A*, close-up stereo view of the active site of inactivated *cis*-CaaD showing the interaction of the carboxylate of the (*R*)-2-hydroxypropanoate adduct with the two arginines (Arg-70 and Arg-73) and histidine (His-28). *B*, close-up stereo view of the active site of inactivated CaaD (5) showing the interaction of the carboxylate group of the 3-oxopropanoate adduct with the two arginines (αArg-8 and αArg-11). *Dark-colored chains* represent the β-chains of the heterohexameric CaaD, whereas the *light-colored chains* represent the α-chains. In both figures, residues are labeled by their chain color, except Pro-1, which is labeled in *black*. The figures were made using MOLSCRIPT and RASTER3D (24, 25).

monomers of *cis*-CaaD and MSAD are structurally the most similar: in a pairwise alignment 97 out of 129 (MSAD) and 147 (*cis*-CaaD) C_α atoms align with an r.m.s.d. value of 1.3 Å. A structural alignment further shows that the two connected β-α-β structural motifs in *cis*-CaaD, and the α- and β-chains of CaaD align with r.m.s.d. values of 0.9 Å for 50 C_α atoms out of a total of 55–62 amino acids. Thus, even though CaaD and *cis*-CaaD belong to different families of the tautomerase superfamily, *cis*-CaaD and CaaD are structurally very similar.

*Structure of cis-CaaD Inactivated by (R)-**8***—It has previously been shown that *cis*-CaaD is inactivated by the active site-directed irreversible inhibitor, (*R*)-**8** (10). In contrast, the (*S*)-enantiomer of **8** is only a weak competitive inhibitor with a K_i value of 9.2 ± 0.8 mM (10). Mass spectral analysis of *cis*-CaaD inactivated by (*R*)-**8** showed that the sole site of modification on the enzyme is Pro-1, and that the increase in molecular mass for the inactivated *cis*-CaaD is consistent with covalent modification by a 2-hydroxypropanoate species. The crystal structure of the inactivated *cis*-CaaD was determined to 2.1-Å resolution by the molecular replacement method using the atomic coordinates for one heterodimer subunit in the heterohexameric CaaD and refined to R and R_{free} values of 20.2% and 23.0%, respectively.

The electron-density map of the inactivated *cis*-CaaD clearly established a covalent linkage between the Pro-1 nitrogen and C3 of the ring opened (*R*)-**8** and allowed an unambiguous determination of the nature of the covalent adduct (Fig. 2*B*). Electron density extends from Pro-1 with an angle that is consistent with a tetrahedral conformation at the prolyl nitrogen, indicating a single bond between the prolyl nitrogen and the C3 atom of the adduct. The prolyl nitrogen is within hydrogen bonding distance (2.8 Å) of the backbone carbonyl oxygen of Leu-38, showing that the prolyl nitrogen is protonated and thus positively charged. Attack at C3 of (*R*)-**8** by Pro-1 places a hydroxyl group at C2 (10). Accordingly, the electron-density map shows electron density consistent with an oxygen atom attached to the second carbon atom (C2) of the adduct, that is at hydrogen bonding distance (3.0 Å) from a water molecule bound to Arg-70. Additional electron density, consistent with a carboxylate group, extends toward the side chains of His-28 and Arg-73. On the basis of these observations, it is concluded that Pro-1 attacked the C3 position of (*R*)-**8** to result in the attachment of (*R*)-2-hydroxypropanoate to the prolyl nitrogen.

*The Active Site of cis-CaaD Inactivated by (R)-**8***—The (*R*)-2-hydroxypropanoate carboxylate group occupies a similar position as the sulfate/phosphate ion in the native structure and makes similar interactions (Figs. 2*A* and 3*A*). It makes two hydrogen bonds (~3.0 Å) with the side-chain guanidinium group of Arg-73 and one hydrogen bond with the backbone nitrogen of Arg-70. In addition, it forms a hydrogen bond (2.7 Å) with the ϵ-nitrogen of His-28. The 2-hydroxyl group of the adduct interacts with the water molecule bound to the side chain of Arg-70 and the hydroxyl group of Thr-34 (not shown). The catalytic base Glu-114 makes a hydrogen bond (2.5 Å) with the side-chain hydroxyl group of Tyr-103′ (Fig. 3*A*) and is rotated with respect to its position in the native structure of *cis*-CaaD. As a result, the other carboxylate oxygen atom of Glu-114 does not interact anymore with the backbone carbonyl group of Leu-38 but instead interacts with a water molecule located approximately at the position of Leu-119 in the native structure. Leu-119 is one of the 22 C-terminal residues that are

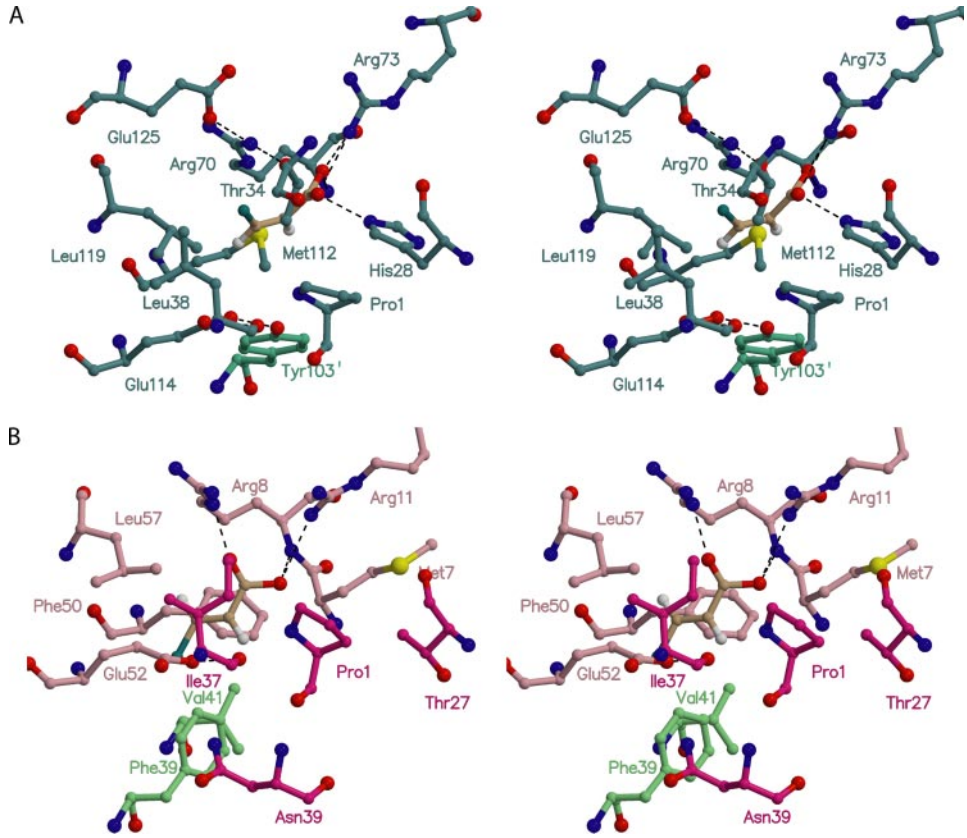

FIGURE 4. **Detailed overviews of modeled substrates bound in the active sites of *cis*-CaaD and CaaD.** *A*, close-up stereo view of the active site of *cis*-CaaD with a modeled *cis*-3-chloroacrylate substrate (*i.e.* **1**) bound by the two arginines (Arg-70 and Arg-73) and histidine (His-28). The orientation of **1** suggests that the 3-chloro substituent interacts with a hydrophobic patch formed by Thr-34, Leu-38, and Leu-119. *B*, close-up stereo view of the active site of CaaD (5) with a modeled *trans*-3-chloroacrylate substrate (*i.e.* **2**) bound by the two arginines (αArg-8 and αArg-11). In this orientation, the 3-chloro substituent interacts with a hydrophobic patch formed by αPhe-39 and αPhe-50. In the figure, the *dark-colored residues* belong to the β-chains of CaaD, whereas the *light-colored residues* belong to the α-chains. In both figures, residues are labeled by their chain color. The figures were made using MOLSCRIPT and RASTER3D (24, 25).

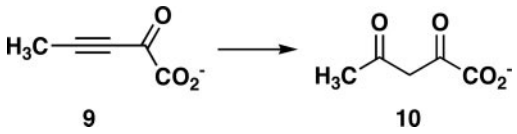

9 **10**

SCHEME 2

not visible in the electron-density maps of the inactivated *cis*-CaaD structure. It remains unclear whether the unstructured C terminus of the inactivated enzyme is due to inactivation of the enzyme by (*R*)-**8** or to a crystallization artifact. Despite this, and given the pH at which the inactivated enzyme was crystallized (pH 7.5), Glu-114 is likely not protonated and in a position to activate the nucleophilic water molecule (see below).

Differences between the cis-CaaD and CaaD Active Sites—The *cis*-CaaD active site shows two significant differences compared with that of CaaD inactivated by 3-bromopropiolate (PDB entry 1S0Y, Fig. 3*B*) (5). The first difference is the presence of a new residue, His-28, involved in the binding of the carboxylate group of the covalent adduct. Significantly, His-28 is conserved in the four sequences included in the *cis*-CaaD family (1). In CaaD, the equivalent position is occupied by a threonine (βThr-27). Second, the active site of *cis*-CaaD has a tyrosine residue (Tyr-103′) that directly interacts with Glu-114. Although the tyrosine is not conserved and is present in only two of the four *cis*-CaaD family sequences (1), its proximity to Glu-114 and the Pro-1 nitrogen suggests that it may have a catalytic role, *e.g.* assisting Glu-114 in the activation of the catalytic water molecule. Indeed, mutation of Tyr-103′ has an effect on enzyme activity (see below). Moreover, the presence of His-28 and Tyr-103′ in *cis*-CaaD, but not in CaaD, could account for the individual substrate specificities.

Structural Basis for the Substrate Specificity of cis-CaaD—A comparison of the structures of *cis*-CaaD and CaaD offers an explanation for their different substrate specificities (Fig. 4). In *cis*-CaaD, the carboxylate group of the substrate is bound by the His-28/Arg-70/Arg-73 cluster, such that the rest of the substrate in the active site is oriented toward the surface of the enzyme (Fig. 4*A*). In CaaD, the carboxylate group of the substrate is bound by the αArg-8/αArg-11 pair, with the remainder of the substrate projecting deeper into the active site (Fig. 4*B*). Thus, the presence of an additional carboxylate-binding residue (His-28) in *cis*-CaaD results in differences in the orientation of the substrate in the active site with respect to CaaD. The substrate-binding pockets fit the shape of their respective substrates (*cf.* **1** and **2**), the pocket of *cis*-CaaD being more U-shaped, whereas the pocket of CaaD is more elongated in shape. One of the residues responsible for this shape difference is Tyr-103′ (αVal-41 in CaaD). In CaaD, αVal-41 creates a hydrophobic region allowing the 3-chloro moiety of the substrate to bind between αPhe-39 and αPhe-50. The presence of the larger Tyr-103′ residue in *cis*-CaaD effectively blocks the binding of the 3-chloro group of a *trans*-substrate. Instead, a pocket formed by the side chains of Thr-34, Leu-38, Leu-119, and Arg70 could favor the binding of the 3-chloro moiety of a *cis*-substrate. Thus, His-28 and Tyr-103′ in *cis*-CaaD appear to be two determinants of the specificity of the enzyme.

The different shapes of the active site pockets may also be responsible for the different efficiencies of CaaD and *cis*-CaaD in hydrating 2-oxo-3-pentynoate (**9**, Scheme 2) (1, 3). Both enzymes convert **9** to acetopyruvate (**10**), but the k_{cat}/K_m of CaaD is ~580-fold higher than that of *cis*-CaaD for this reaction. The higher value is due to a ~100-fold greater k_{cat} combined with a ~5.6-fold lower K_m (1, 3). The linear acetylene molecule is evidently accommodated more easily by the elongated active site of CaaD than it is by the U-shaped active site of *cis*-CaaD, as suggested by the different K_m values. If **9** binds to

TABLE 2
Kinetic parameters for *cis*-CaaD and mutant proteins using 1

Enzyme	k_{cat}	K_m	k_{cat}/K_m
	s^{-1}	μM	$s^{-1}\,M^{-1}$
cis-CaaD[a]	1.7 ± 0.1	55 ± 6	3.1×10^4
E114Q	0.020 ± 0.006	4.3 ± 0.2	4.6×10^3
Y103F	0.13 ± 0.02	2.4 ± 1.1	5.4×10^4

[a] The steady-state kinetic parameters were determined in 20 mM Na_2HPO_4 buffer (pH 9.0) at 23 °C. Errors are standard deviations. There was no detectable activity for the H28A or the Y103F/E114Q mutant proteins.

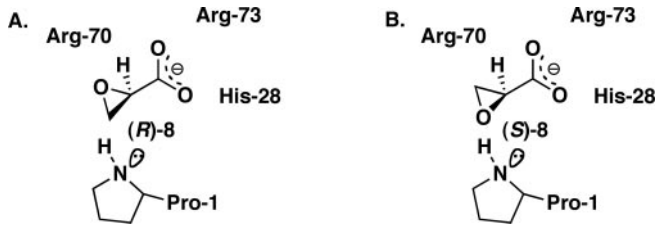

SCHEME 3

CaaD in an orientation similar to that proposed for **2**, then the linear acetylene molecule would be directed into the active site. In this proposed binding mode, the two arginine residues of CaaD would interact with the 2-carbonyl oxygen as well as one or both carboxylate oxygens of **9**. If **9** binds to *cis*-CaaD in a comparable mode to that proposed for **1**, the linear acetylene molecule would now be directed into the U-shaped cavity. Such an orientation would not be a favorable one and may preclude efficient binding and catalysis. The presence of Tyr-103′ may also interfere with the binding of **9**.

Mutagenesis of His-28 and Tyr-103′—To investigate the importance of Tyr-103′ and His-28 for the dehalogenation reaction, the H28A, Y103F, and Y103F/E114Q mutants of *cis*-CaaD were made and purified. Determination of their kinetic parameters and comparison with the wild type and E114Q-*cis*-CaaD activities showed that His-28 is essential for catalytic activity, because the H28A mutant has no detectable activity in the kinetic assay. Glu-114 is more important than Tyr-103′ as assessed by their k_{cat} values (Table 2), but neither one is as critical as His-28. However, the Glu-114/Tyr-103′ pair is necessary as indicated by the observation that the Y103F/E114Q mutant has no detectable activity in the kinetic assay. Thus, it can be concluded that the three residues His-28, Tyr-103′, and Glu-114 are important for the *cis*-CaaD-catalyzed dehalogenation of **1**.

To assess the relative importance of the six active site residues identified to date (Pro-1, His-28, Arg-70, Arg-73, Tyr-103′, and Glu-114) to *cis*-CaaD activity, the reactions catalyzed by the individual mutant proteins (P1A, H28A, R70A, R73A, Y103F, and E114Q) and the double mutant protein (Y103F/E114Q) were examined by ^{1}H NMR spectroscopy at 17 or 22 h, and the amount of product was quantified. Both the Y103F- and E114Q-catalyzed reactions were 100% complete at 17 h, whereas the H28A-catalyzed reaction was only 85% complete at 22 h. In contrast, the R70A-catalyzed reaction showed only a trace of product, the R73A reaction mixture generated ~1% product, and the P1A reaction mixture yielded ~4% product at 17 h. The reaction mixture containing the double mutant protein (Y103F/E114Q) resulted in ~6% product (at 17 h). The NMR analysis, which is consistent with the kinetic data reported here and elsewhere (1), suggests that Pro-1, Arg-70, and Arg-73 are the most essential catalytic residues in *cis*-CaaD. Hence, substrate activation and protonation at C2 may be more critical for the dehalogenation reaction than the activation of water.

*Mechanism of Inactivation of cis-CaaD by (R)-**8***—It has previously been shown that inactivation of *cis*-CaaD by (*R*)-**8** requires Pro-1, Arg-70, and Arg-73 (10). In contrast, the E114Q mutant protein is alkylated by (*R*)-**8** indicating that Glu-114 is not essential for the inactivation reaction. These observations are consistent with a mechanism for covalent modification involving the nucleophilic attack of Pro-1 at C2 or C3 of (*R*)-**8** concomitant with the formation of a hydrogen bond between the oxirane oxygen and a nearby proton donor or protonation of the oxirane oxygen by a proton source (10).

The present crystal structure of the inactivated *cis*-CaaD establishes the C3 position of (*R*)-**8** as the site of nucleophilic attack by Pro-1. The structure also shows that the carboxylate group of the adduct interacts with the side chains of His-28, Arg-73, and the backbone nitrogen atom of Arg-70 (Fig. 3*A*). The side chain of Arg-70 interacts only indirectly, via a water molecule, with the hydroxyl and carboxylate groups of the inhibitor. These observations suggest that Arg-73 and His-28 are predominantly involved in the binding of the carboxylate group and that Arg-70 may facilitate ring opening by direct interaction with the epoxide oxygen or by placing a water molecule in position to interact with the epoxide oxygen. Furthermore, the interactions of Arg-70 and the His-28/Arg-73 pair with the covalent adduct suggest that prior to inactivation (*R*)-**8** was positioned in the active site with the oxirane oxygen near Arg-70 and the C3 atom proximal to Pro-1 (Scheme 3*A*). If the (*S*)-enantiomer of **8** binds to *cis*-CaaD with similar interactions between the carboxylate group and Arg-73 and His-28, the C3 carbon atom would be directed away from Pro-1 and toward Arg-70 (Scheme 3*B*). This binding mode precludes alkylation of Pro-1 but could result in competitive inhibition, which has been observed experimentally (10).

The proposed binding mode also provides a reasonable explanation for the fact that CaaD is not inactivated by either enantiomer of **8**. CaaD lacks His-28 (or an equivalent) in the active site so that the carboxylate group of **8** might interact with both arginines (in this case, αArg-8 and αArg-11), similar as observed in the crystal structure of inactivated CaaD (Fig. 3*B*). Because both arginines are now involved in binding the carboxylate group, this would prevent one of the arginines from functioning as the required proton donor assisting in the ring opening reaction of the epoxide moiety. Such a binding mode could again lead to competitive inhibition, which has been observed experimentally. This analysis implicates His-28 as a critical residue that makes *cis*-CaaD, but not CaaD, subject to irreversible inhibition.

*Mechanism of the Dehalogenation of **1***—The crystallographic observations and mutagenesis results described above along with work discussed elsewhere (1) identify and establish the relative importance of Pro-1, His-28, Arg-70, Arg-73, Tyr-103′, and Glu-114 in the *cis*-CaaD catalytic mechanism (Scheme 4). The mechanism can be broken down into three components:

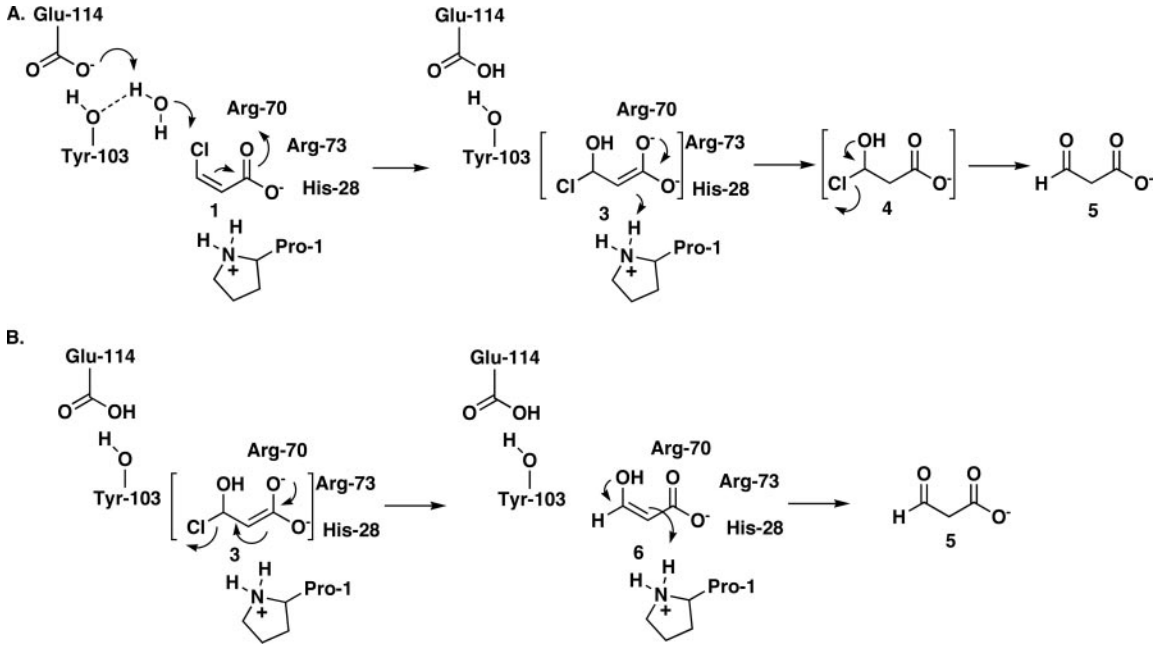

SCHEME 4

activation of water by Glu-114 and Tyr-103′; activation and alignment of substrate by His-28, Arg-70, and Arg-73; and protonation at C2 by Pro-1. Our results show that the individual contributions of the residues in substrate activation and protonation are more important to catalysis than those involved in the activation of water.

The structures of the native and inactivated enzyme suggest that Tyr-103′ is in a position to assist Glu-114 in the activation of a water molecule for attack at C3 of **1**. A specific role cannot be assigned to Tyr-103′, but three possibilities exist. Tyr-103′ can position the water molecule or the carboxylate group of Glu-114, assist in activation of the water molecule (as shown in Scheme 4), or any possible combination. All of these roles are consistent with the diminished k_{cat} of the Y103F mutant protein, but the function of Glu-114 is clearly more important than that of Tyr-103′ in water activation. Removing both residues does, however, severely compromise *cis*-CaaD activity.

The structures also suggest that the His-28/Arg-70/Arg-73 cluster assists in the binding and activation of the substrate by interacting with the oxygen atoms of the C-1 carboxylate group. The three residues likely polarize the carboxylate group, which results in a partial positive charge at C3, which, in turn, facilitates the addition of water. The specific interactions between the His-28/Arg-70/Arg-73 cluster and the carboxylate group are not known, but they may parallel those observed in the structure of the inactivated enzyme (Fig. 3*A*). The individual contributions of Arg-70 and Arg-73 are clearly essential for activity, while that of His-28 is less so.

After water addition, the enzyme-stabilized enediolate intermediate **3** can undergo two equally plausible fates (Scheme 4, *A* and *B*) (1, 10). As shown in Scheme 4*A*, enediolate **3** can ketonize with protonation at C2 by Pro-1. The resulting chlorohydrin intermediate (*i.e.* **4**) can then undergo an enzyme-catalyzed or a non-enzymatic process to produce **5**. Alternatively, enediolate **3** can ketonize with elimination of the chloride ion (Scheme 4*B*). Ketonization of **6** and protonation at C2 by Pro-1 yields **5**. The available data do not allow us to favor one pathway over the other, but the protonation step is an essential component of both, with a key feature being the pK_a of Pro-1. The pH rate profile of *cis*-CaaD implicates a group on the free enzyme with a pK_a of 9.3 (10), similar to what has been found for CaaD (a pK_a of 9.2). Although in CaaD the group with the pK_a of 9.2 was assigned to β-Pro-1 by NMR titration, such an assignment has not been done for *cis*-CaaD. However, like that of CaaD, the environment of Pro-1 in *cis*-CaaD is consistent with such a pK_a, with the presence of the charged and polar side chains of Glu-114 and Tyr-103′ to stabilize the positive charge on the Pro-1 nitrogen atom. Thus, the observed environment of Pro-1 is in agreement with a role as a general acid catalyst.

Evolutionary Implications—The conservation of the β-α-β building block and the four essential catalytic residues suggests that CaaD and *cis*-CaaD are related by divergent evolution from a common ancestor. The different oligomer structures and low sequence identity would further suggest that the two enzymes diverged quite some time ago. Two scenarios can be envisioned: in one, *cis*-CaaD evolved from a direct ancestor of CaaD, whereas in the other, CaaD and *cis*-CaaD evolved independently. A gene duplication event of a small gene encoding the β-α-β structural motif followed by co-evolution of the two genes could give rise to CaaD. *cis*-CaaD could then have diverged from these two genes (and thus from the direct ancestor of CaaD), by a second duplication event of the two genes followed by gene fusion. In this scenario, the two enzymes have a single evolutionary lineage. Alternatively, *cis*-CaaD might have evolved from an independent gene duplication event of the small gene followed by gene fusion. In this scenario, CaaD and *cis*-CaaD evolved independently. The presence of His-28 and Tyr-103′ in the *cis*-CaaD active site and the low sequence identity between CaaD and *cis*-CaaD implicate the second scenario, which is consistent with our previously reported phylo-

genetic analysis (1). Hence, the last common ancestor of CaaD and *cis*-CaaD was probably a small gene encoding the β-α-β structural motif.

REFERENCES

1. Poelarends, G. J., Serrano, H., Person, M. D., Johnson, Jr., W. H., Murzin, A. G., and Whitman, C. P. (2004) *Biochemistry* **43,** 759–772
2. Poelarends, G. J., Saunier, R., and Janssen, D. B. (2001) *J. Bacteriol.* **183,** 4269–4277
3. Wang, S. C., Person, M. D., Johnson, W. H., Jr., and Whitman, C. P. (2003) *Biochemistry* **42,** 8762–8773
4. Azurmendi, H. F., Wang, S. C., Massiah, M. A., Poelarends, G. J., Whitman, C. P., and Mildvan, A. S. (2004) *Biochemistry* **43,** 4082–4091
5. de Jong, R. M., Brugman, W., Poelarends, G. J., Whitman, C. P., and Dijkstra, B. W. (2004) *J. Biol. Chem.* **279,** 11546–11552
6. Poelarends, G. J., Wilkens, M., Larkin, M. J., van Elsas, J. D., and Janssen, D. B. (1998) *Appl. Environ. Microbiol.* **64,** 2931–2936
7. Murzin, A. G. (1996) *Curr. Opin. Struct. Biol.* **6,** 386–394
8. Whitman, C. P. (2002) *Arch. Biochem. Biophys.* **402,** 1–13
9. Poelarends, G. J., and Whitman, C. P. (2004) *Bioorg. Chem.* **32,** 376–392
10. Poelarends, G. J., Serrano, H., Person, M. D., Johnson, Jr., W. H., and Whitman, C. P. (2004) *Biochemistry* **43,** 7187–7196
11. Petit, Y., and Larcheveque, M. (1998) *Organic Syntheses* **75,** 37–44
12. Sambrook, J., Fritsch, E. F., and Maniatis, T. (1989) *Molecular Cloning: A Laboratory Manual*, Cold Spring Harbor Laboratory, Cold Spring Harbor, NY
13. Laemmli, U. K. (1970) *Nature* **227,** 680–685
14. Waddell, W. J. (1956) *J. Lab. Clin. Med.* **48,** 311–314
15. Otwinowski, Z., and Minor, W. (1997) *Methods Enzymol.* **276,** 307–326
16. Navaza, J., and Saludjian, P. (1997) *Methods Enzymol.* **276,** 581–594
17. Collaborative Computational Project, Number 4. (1994) *Acta Crystallogr. Sect. D Biol. Crystallogr.* **50,** 760–763
18. Read, R. J. (1986) *Acta Crystallogr. Sect. A* **42,** 140–149
19. Terwilliger, T. C. (2001) *Acta Crystallogr. Sect. D Biol. Crystallogr.* **57,** 1763–1775
20. McRee, D. E. (1999) *J. Struct. Biol.* **125,** 156–165
21. Kjeldgaard, M., and Jones, T. A. (1998) *Acta Crystallogr. Sect. D Biol. Crystallogr.* **54,** 1119–1131
22. Laskowski, R. A., MacArthur, M. W., Moss, D. S., and Thornton, J. M. (1993) *J. Appl. Crystallogr.* **26,** 283–291
23. Ho, S. N., Hunt, H. D., Horton, R. M., Pullen, J. K., and Pease, L. R. (1989) *Gene* (*Amst.*) **77,** 51–59
24. Kraulis, P. J. (1991) *J. Appl. Crystallogr.* **24,** 946–950
25. Merritt, E. A., and Murphy, M. E. (1994) *Acta Crystallogr. Sect. D Biol. Crystallogr.* **50,** 869–873
26. Almrud, J. J., Kern, A. D., Wang, S. C., Czerwinski, R. M., Johnson, W. H., Jr., Murzin, A. G., Hackert, M. L., and Whitman, C. P. (2002) *Biochemistry* **41,** 12010–12024
27. Poelarends, G. J., Johnson, W. H., Jr., Murzin, A. G., and Whitman, C. P. (2003) *J. Biol. Chem.* **278,** 48674–48683
28. Sparnins, V. L., Chapman, P. J., and Dagley, S. (1974) *J. Bacteriol.* **120,** 159–167
29. Harayama, S., Rekik, M., Ngai, K.-L., and Ornston, L. N. (1989) *J. Bacteriol.* **171,** 6251–6258
30. Rosengren, E., Aman, P., Thelin, S., Hansson, C., Ahlfors, S., Bjork, P., Jacobsson, L., and Rorsman, H. (1997) *FEBS Lett.* **417,** 85–88
31. Subramanya, H. S., Roper, D. I., Dauter, Z., Dodson, E. J., Davies, G. J., Wilson, K. S., and Wigley, D. B. (1996) *Biochemistry* **35,** 792–802
32. Taylor, A. B., Johnson, Jr., W. H., Czerwinski, R. M., Li, H.-S., Hackert, M. L., and Whitman, C. P. (1999) *Biochemistry* **38,** 7444–7452
33. Almrud, J. J., Poelarends, G. J., Johnson, W. H., Jr., Serrano, H., Hackert, M. L., and Whitman, C. P. (2005) *Biochemistry* **44,** 14818–14827